

**OPEN ACCESS**

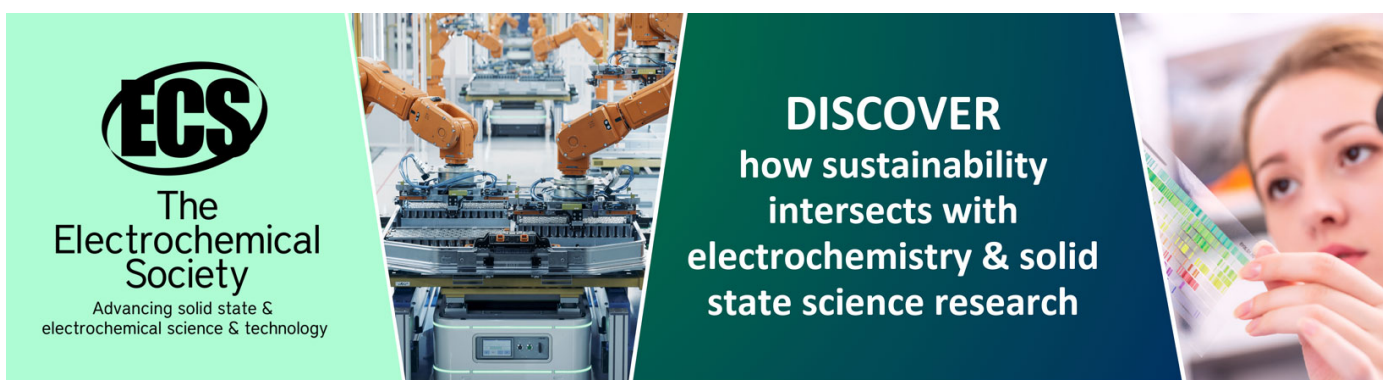
## Activation Experiments for $p$ -Process Nucleosynthesis

To cite this article: K Sonnabend *et al* 2011 *J. Phys.: Conf. Ser.* **312** 042007

View the [article online](#) for updates and enhancements.

### You may also like

- [3D Mapping of plasma effective areas via detection of cancer cell damage induced by atmospheric pressure plasma jets](#)  
Xu Han, Yueing Liu, M Sharon Stack et al.
- [THE  \$^{12}\text{C} + ^{12}\text{C}\$  REACTION AND THE IMPACT ON NUCLEOSYNTHESIS IN MASSIVE STARS](#)  
M. Pignatari, R. Hirschi, M. Wiescher et al.
- [Study of elastic collisions of \*Myxococcus xanthus\* in swarms](#)  
Cameron W Harvey, Faruck Morcos, Christopher R Sweet et al.



**ECS**  
The  
Electrochemical  
Society  
Advancing solid state &  
electrochemical science & technology

**DISCOVER**  
how sustainability  
intersects with  
electrochemistry & solid  
state science research

# Activation Experiments for $p$ -Process Nucleosynthesis

**K Sonnabend<sup>1,2,3</sup>, J Glorius<sup>1</sup>, J Görres<sup>2</sup>, M Knörzer<sup>1</sup>, S Müller<sup>1</sup>, A Sauerwein<sup>1,2,3,4</sup>, W P Tan<sup>2</sup>, M Wiescher<sup>2</sup>**

<sup>1</sup> Institut für Kernphysik, TU Darmstadt, Schlossgartenstr. 9, D-64289 Darmstadt, Germany

<sup>2</sup> University of Notre Dame, Department of Physics, Notre Dame, Indiana 46556, U.S.A.

<sup>3</sup> Joint Institute for Nuclear Astrophysics (JINA), U.S.A.

E-mail: [sonnabend@ikp.tu-darmstadt.de](mailto:sonnabend@ikp.tu-darmstadt.de)

**Abstract.** Activation experiments are a perfect tool to perform systematic studies due to their high sensitivity and selectivity. Exemplary applications to understand the nucleosynthesis of the  $p$  nuclei – such as the optimization of optical particle-nucleus potentials and investigations of  $(\gamma, n)$  reactions in a broad mass range – are presented. Some recent and partly preliminary results are briefly discussed.

## 1. Introduction

The nucleosynthesis of the elements above the so-called iron peak in the solar abundance distribution is mainly explained by neutron-capture processes. During stellar burning phases, the slow neutron capture process ( $s$  process) takes place on a time scale of several 10000 years at moderate temperatures of about  $10^8$  K and neutron densities ranging from  $10^6$   $\text{cm}^{-3}$  to  $10^{12}$   $\text{cm}^{-3}$ . Given these conditions, a reaction path is determined by a series of subsequent neutron-capture reactions and  $\beta$  decays that is close to the valley of  $\beta$  stability [1, 2, 3]. In contrast, the rapid neutron-capture process ( $r$  process) happens in explosive scenarios lasting only for a few seconds and producing extreme conditions: Temperatures of more than  $10^9$  K are combined with neutron-densities higher than  $10^{20}$   $\text{cm}^{-3}$ . Thus, very neutron-rich isotopes near the neutron dripline are produced that decay back to the valley of  $\beta$  stability afterwards [4].

However, there are some proton-rich isotopes left that cannot be produced in either of these processes [5]. It is still an outstanding question whether the nucleosynthesis of the so-called  $p$  nuclei can be consistently explained in one astrophysical scenario although it is clear that an explosive environment is needed [6]. Nowadays, it seems to be more likely that different scenarios and, thus, production mechanisms contribute in overlapping mass regions. The light  $p$  nuclei might be dominantly produced in processes dealing with proton-capture reactions such as the  $rp$  process [7] and  $\nu p$  process [8] while the heavier  $p$  nuclei stem from a series of photodisintegrations on a seed of  $r$ - and  $s$ -process nuclei. A likely site for this mechanism that is sometimes referred to as  $\gamma$  process are the O-Ne-layers of type II supernovae [9, 10]. However, recent studies suggest that some of the characteristic  $p$  nuclei can also be produced in charged-particle reactions within the high-entropy wind  $r$  process model [11].

<sup>4</sup> present address: Institut für Kernphysik, Universität zu Köln, Zùlpicher Str. 77, D-50937 Cologne, Germany

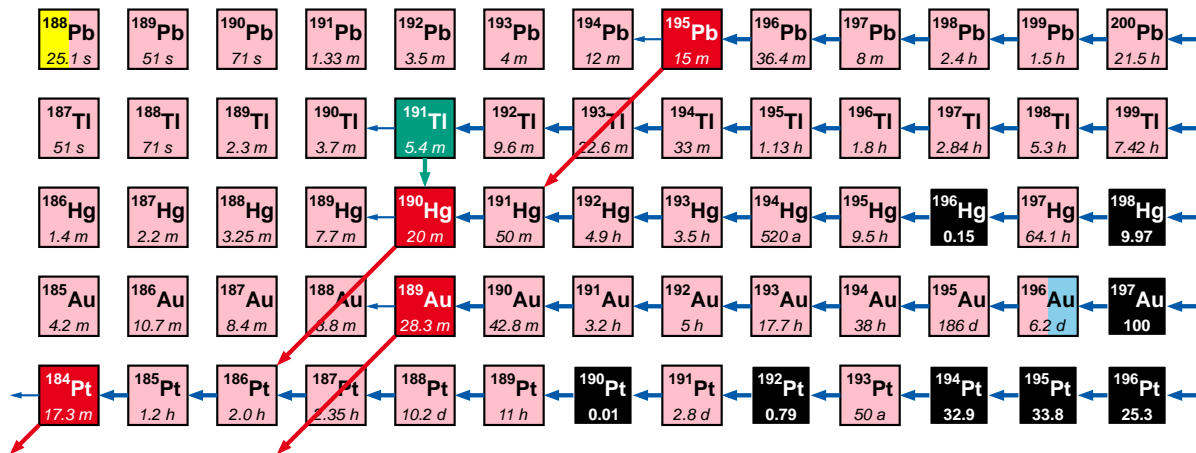


**Figure 1.** Illustration of the reaction network of the  $p$  process on a detail of the chart of nuclides. A number of seed nuclei is photodisintegrated in a series of  $(\gamma, n)$ ,  $(\gamma, p)$ , and  $(\gamma, \alpha)$  reactions. Branchings occur and determine the final abundance distribution if the  $(\gamma, p)$  reaction rate – like at  $^{191}\text{Tl}$  – or the  $(\gamma, \alpha)$  reaction rate – like at  $^{184}\text{Pt}$ ,  $^{189}\text{Au}$ ,  $^{190}\text{Hg}$ , and  $^{195}\text{Pb}$  – becomes close to the  $(\gamma, n)$  reaction rate (data taken from [10]). The time indicated with the unstable nuclei is the laboratory half-life.

To simulate the nucleosynthesis in these conditions, huge reaction networks – like partly shown in Fig. 1 – involving more than 1000 isotopes and more than 10000 reaction rates have to be used. A comparably small number of reactions was found to significantly influence the produced abundance pattern if the reaction rates are varied [9, 10]. However, it will not be possible to measure all of these reactions in the near future, therefore, the prediction of the abundance pattern still depends on the calculation of reliable rates. In addition, excited states are populated in the nuclei due to the high temperatures of several  $10^9$  K so that the ground-state reaction rate has to be significantly corrected based on theoretical predictions.

Since mostly compound nucleus reactions take place, the predictions are performed in the framework of the Hauser-Feshbach model [12]. Thus, the reliability of the input from nuclear physics – such as  $\gamma$ -ray strength functions, optical particle-nucleus potentials, and level densities – is mandatory to achieve secure results [13, 14]. This can be realized by testing the predictions experimentally for selected isotopes and in systematic studies.

A perfect tool for the latter case are activation experiments: their high sensitivity and selectivity allows measurements with small amounts of target material which is mostly the case for the low abundant  $p$  nuclei. The following sections will discuss different approaches for systematic studies: Section 2 is about studies where charged particle induced reactions are involved while Sec. 3 focusses on studies of photon-induced reactions. An outlook to future experimental approaches is presented in Sec. 4.

## 2. Experiments on particle-induced reactions

If charged particle induced reactions are studied the focus is on the determination of optical particle-nucleus potentials. Therefore, the reaction cross section is extracted from the experimental data and compared to the predicted value. Different optical particle-nucleus potentials are used in the prediction to find the best solution with respect to the observed energy dependence and absolute value of the cross section (compare *e.g.* [15]).

The most demanding need is a better description of optical  $\alpha$ -nucleus potentials [13]. Systematic studies using elastic  $\alpha$  scattering were carried out [16, 17, 18, 19]. The results

were compared to and combined with activation measurements of  $\alpha$ -induced reactions such as  $(\alpha,\gamma)$ ,  $(\alpha,p)$ , and  $(\alpha,n)$  (see Fig. 2a, [20]). However, it was not possible to find one optical  $\alpha$ -nucleus potential that describes a complete set of these reactions without significant deviations in one or another of the reactions.

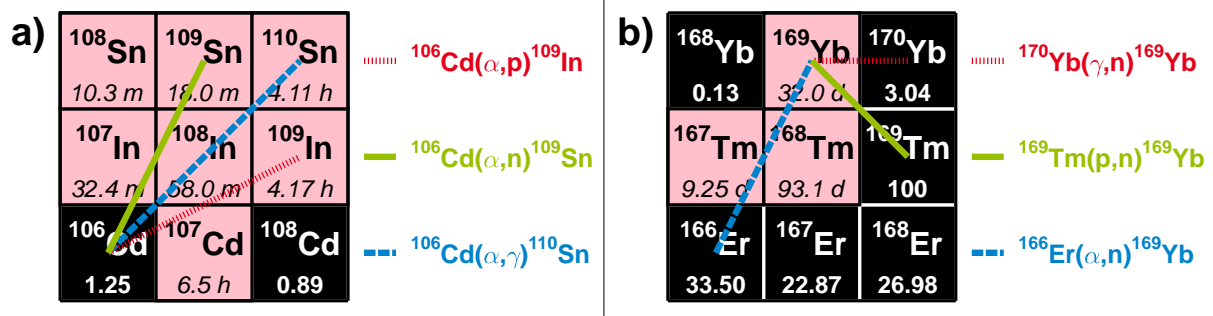


**Figure 2.** Systematic studies on optical particle-nucleus potentials. *left:* All studied reactions are induced by  $\alpha$  particles (see [20]). *right:* The same compound nucleus is produced with different projectiles and its decay by neutron emission is studied.

Another approach using charged particle induced reactions is to focus the attention on reactions with the same decay channel of the compound nucleus and study *e.g.* a combination of  $(\alpha,n)$ ,  $(p,n)$ , and  $(\gamma,n)$  reactions like illustrated in Fig. 2b. The reaction yield  $Y$  is experimentally determined by the number of observed decays  $A$  of the unstable nuclei that were produced during the activation using high-resolution  $\gamma$  spectroscopy:

$$A = \varepsilon_{\gamma} \cdot I_{\gamma} \cdot \tau \cdot \frac{t_L}{t_R} \cdot Y \quad (1)$$

with the detector efficiency  $\varepsilon_{\gamma}$ , the branching factor  $I_{\gamma}$  of the observed decay line, and the dead-time correction  $t_L/t_R$ . The factor  $\tau$  corrects for the continuous decay of produced unstable nuclei during the activation, waiting time and  $\gamma$  spectroscopy. Its detailed composition can be found in *e.g.* [21]. Typical decay spectra are shown in Fig. 3.

In general, the reaction yield  $Y$  is related to the reaction cross section  $\sigma$  by:

$$Y = \mu_T \cdot \int \sigma(E) \cdot N(E) \cdot dE \quad (2)$$

with the number of target atoms per unit area  $\mu_T$  and the number of projectiles as a function of energy  $N(E)$ . For charged particle induced reactions, the projectiles are considered monoenergetic, thus, Eq. (2) becomes:

$$Y = \mu_T \cdot \sigma(E) \cdot N_{p,\alpha} \quad (3)$$

where the total number of incident protons or  $\alpha$  particles  $N_{p,\alpha}$  is usually determined by measuring the current impinging on the target.

In the case of photon-induced reactions,  $\mu_T$  in Eq. (2) has to be replaced by the total number of target atoms  $N_T$  as the beam is broad and covers the complete target area. Thus,  $N(E)$  becomes the number of photons per unit area and energy. If continuous-energy bremsstrahlung is used the cross section  $\sigma$  can only be determined for the complete energy range of the bremsstrahlung spectrum. Thus, an energy-integrated cross section  $I_{\sigma}$  is usually introduced and Eq. (2) becomes:

$$Y = N_T \cdot I_{\sigma}(E_{\max}) = N_T \int_S^{E_{\max}} \sigma(E) \cdot N_{\gamma}^{\text{brems}}(E, E_{\max}) \cdot dE \quad (4)$$

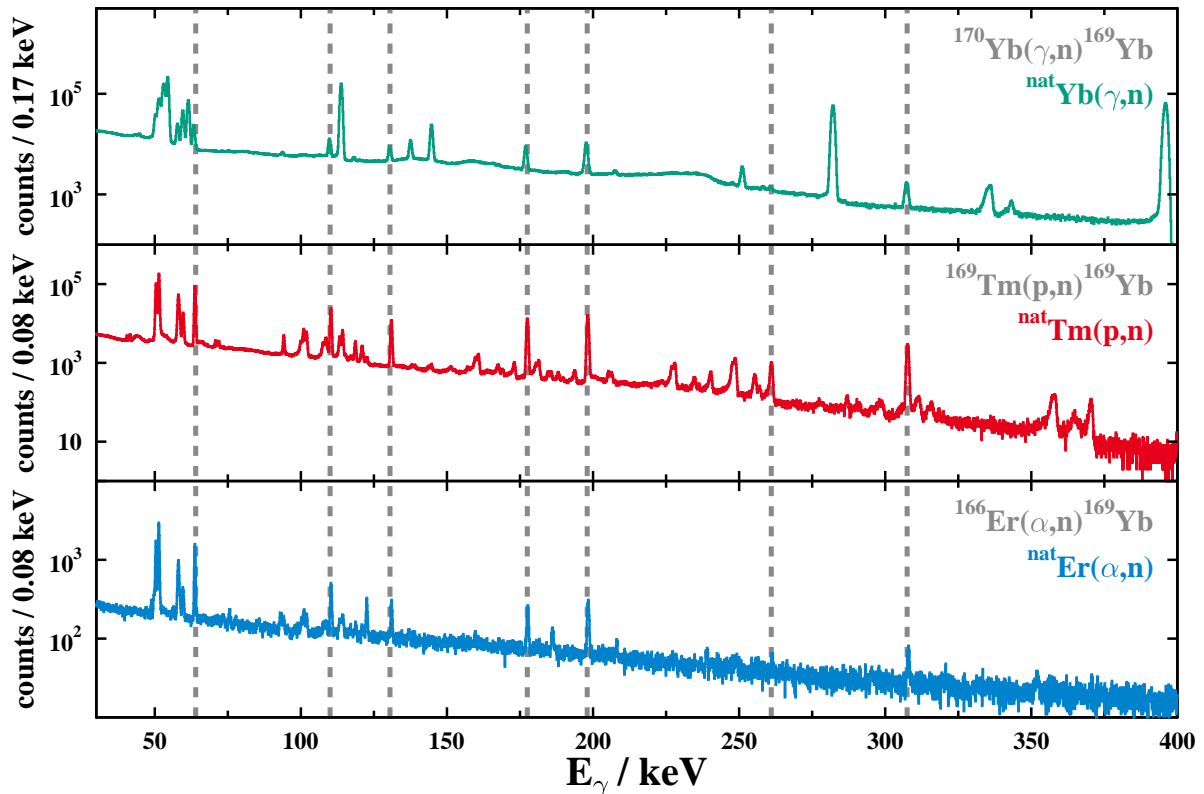


**Figure 3.** Typical decay spectra after activation experiments. The dashed grey lines indicate the peaks corresponding to  $\gamma$  transitions in the decay of  $^{169}\text{Yb}$ . *top:* Spectrum measured after the activation of naturally composed Ytterbium with bremsstrahlung. Non-marked peaks stem from the decays of  $^{167}\text{Yb}$  and  $^{175}\text{Yb}$ . In addition, x-rays occur at low energies [22]. *middle:* Spectrum measured after the activation of  $^{169}\text{Tm}$  with protons. All structures are due to the decay of  $^{169}\text{Yb}$ . Non-marked peaks stem from accidental coincidences due to high count rates and a close geometry of target and detector. *bottom:* Spectrum measured after the activation of naturally composed erbium with  $\alpha$  particles. Non-marked peaks stem from small impurities in the target material such as iron that led to the production of *e.g.*  $^{57}\text{Co}$ . Details on the analysis of the target material can be found in [23].

with the reaction threshold  $S$ , the maximum energy of the bremsstrahlung distribution  $E_{\text{max}}$ , and the number of photons per unit area and energy  $N_{\gamma}^{\text{brems}}(E, E_{\text{max}})$ .

Since the different cross sections of the reaction triplet introduced above are calculated from an analysis of the same decay the systematic uncertainties are significantly reduced using this approach.

We have performed experiments on the reactions  $^{166}\text{Er}(\alpha, n)$  and  $^{169}\text{Tm}(p, n)$  at the FN Tandem Accelerator System of the University of Notre Dame. The aim was to measure at lowest energies to be as close to the Gamow window corresponding to  $p$ -process nucleosynthesis as possible. Thus, the energies of the  $\alpha$  beam were chosen between 15 MeV and 11.75 MeV in the laboratory frame resulting in activation times of 2 h up to 3 d while the proton beam was used with energies ranging from 7 MeV down to 3.3 MeV in the laboratory frame for activation times between 2 h and 2.5 d. The  $\gamma$  spectroscopy was performed after the activation using four different setups of High-Purity Germanium (HPGe) detectors at the University of Notre Dame

and at the Technische Universität Darmstadt, respectively. All HPGe detectors were shielded passively against natural background mounting lead and copper around the crystals. The energy and efficiency calibration was performed with standard calibration sources.

Figure 4 shows the cross sections extracted from spectra like shown in Fig. 3. The experimental values of the  $(\alpha,n)$  and  $(p,n)$  reaction cross sections are compared to the predictions of the NON-SMOKER [13] and TALYS [24] codes. In both cases, the energy dependence predicted by NON-SMOKER is in better agreement to the experimental data. However, the absolute discrepancy of about a factor of 6 in case of the  $(\alpha,n)$  reaction calls for further analysis.

An idea is to measure also the reaction  $^{165}\text{Ho}(\alpha,n)$  that proceeds via the neighbored compound nucleus  $^{168}\text{Tm}$ . If a comparable discrepancy of the predicted cross sections and the experimental result occurs the data should be used to establish a local description of an optical  $\alpha$ -nucleus potential. After cross-checking its validity with other data measured in that mass region its influence on the  $p$ -process abundances has to be determined.

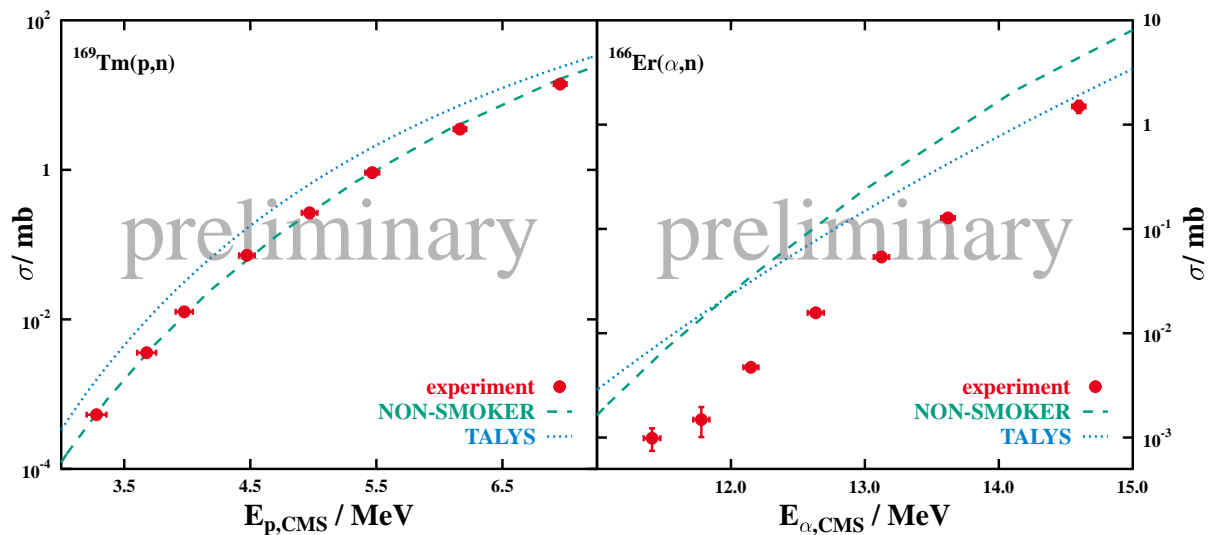


**Figure 4.** Comparison of experimental and predicted cross sections. The red dots are the experimentally derived values. The green-dashed and blue-dotted lines describe the prediction of the Hauser-Feshbach codes NON-SMOKER [13] and TALYS [24], respectively. *left:* Cross section of the reaction  $^{169}\text{Tm}(p,n)$ . The energy dependence is well described by both predictions but only the NON-SMOKER code provides also reasonable absolute values. *right:* Cross section of the reaction  $^{166}\text{Er}(\alpha,n)$ . Both predictions cannot reproduce the measured values. The energy dependence predicted by the NON-SMOKER code is reasonable but the absolute value is about a factor of 6 too high.

### 3. Experiments on photon-induced reactions

Since most of the  $p$  nuclei are produced in series of photodisintegrations it is also interesting to study  $(\gamma,n)$ ,  $(\gamma,p)$ , and  $(\gamma,\alpha)$  reactions. Measurements were performed with continuous-energy bremsstrahlung photons [25, 26, 27, 28, 29] and quasi-monoenergetic photons from Laser Compton Backscattering (LCB) [30, 31, 32] (see [33] as review). In near future, also tagged photons will be available with high energy resolution in the astrophysically relevant energy range at the low-energy photon tagger NEPTUN at the S-DALINAC, Darmstadt [34, 35].

Using bremsstrahlung photons, the ground-state reaction rate can be deduced from a series of activations without any assumption on the energy dependence of the cross section [21].

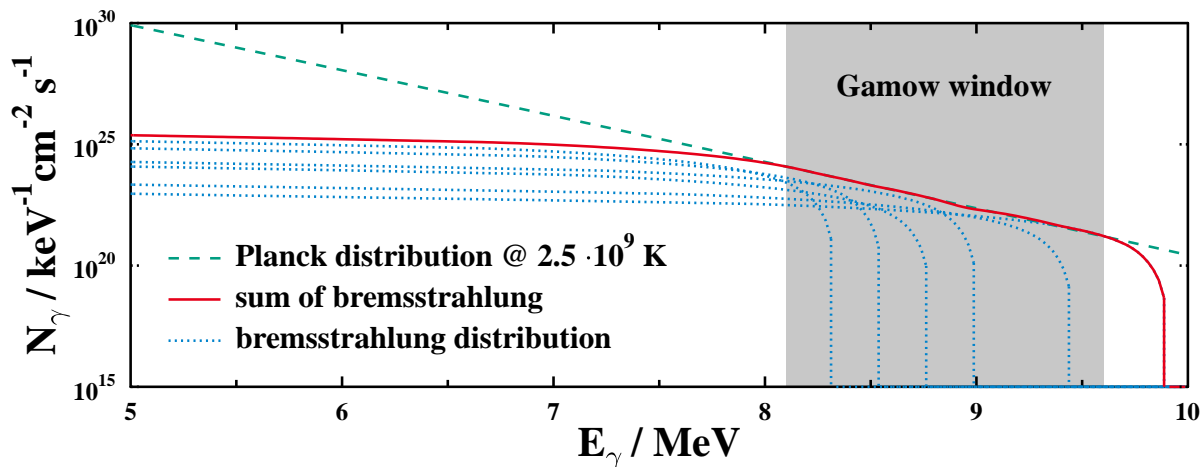


**Figure 5.** Approximation of a Planck distribution by bremsstrahlung spectra. The exponential tail of a Planck distribution  $n_{\text{Planck}}$  at a temperature of  $2.5 \cdot 10^9$  K is shown (green-dashed line) in the energy range of 5 MeV to 10 MeV. The red-solid line is the sum of several bremsstrahlung distributions  $N_{\gamma,i}^{\text{brems}}(E, E_{\text{max},i})$  (blue-dotted lines) with different maximum energies  $E_{\text{max},i}$  and approximates the Planck distribution in the grey shaded area. This so-called Gamow window indicates the energy range where the knowledge of the  $(\gamma, n)$  reaction for an example nucleus with a neutron separation threshold of 8.1 MeV is important for  $p$ -process nucleosynthesis at the given temperature.

Therefore, the Planck distribution  $n_{\text{Planck}}$  at typical  $p$ -process temperatures is approximated by a sum of bremsstrahlung spectra  $N_{\gamma}^{\text{brems}}(E, E_{\text{max},i})$  that are weighted with temperature dependent factors  $a_i(T)$  to reproduce the Planck distribution in the corresponding Gamow window of the reaction as shown in Fig. 5.

Since the reaction rate  $\lambda$  for a photon-induced reaction is given by:

$$\lambda(T) = \int c \cdot n_{\text{Planck}}(T) \cdot \sigma(E) \cdot dE \quad (5)$$

and the Planck distribution  $n_{\text{Planck}}$  is approximated by:

$$c \cdot n_{\text{Planck}}(T) \approx \sum a_i(T) \cdot N_{\gamma,i}^{\text{brems}}(E, E_{\text{max},i}) \quad (6)$$

the reaction rate can be rewritten using Eqs. (1) and (4) to:

$$\lambda(T) \propto \sum a_i(T) \cdot A(E_{\text{max},i}). \quad (7)$$

Using Eq. (7), the reaction rate  $\lambda$  at a given temperature  $T$  is directly derived from the peak areas  $A(E_{\text{max},i})$  in the measured decay spectra (compare top panel of Fig. 3). However, the data are derived under laboratory conditions so that no excited states are populated in the target nuclei. Therefore, it is more appropriate to call the results derived with this method ground-state reaction rates.

Figure 6 shows the results of the measurements we performed at the Darmstadt High-Intensity Photon Setup (DHIPS) [36] during the last years. A comparison of such ground-state reaction rates to the predicted values with the standard settings of the TALYS code [24] in the mass region of  $140 \leq A \leq 210$  is provided. No systematic deviations were found, however, there are several isotopes where the deviation is bigger than the normally stated accuracy of the predictions. In addition, to resolve these problems, it is needed to check the dependence of the accuracy on the variation of the relevant nuclear physics input.

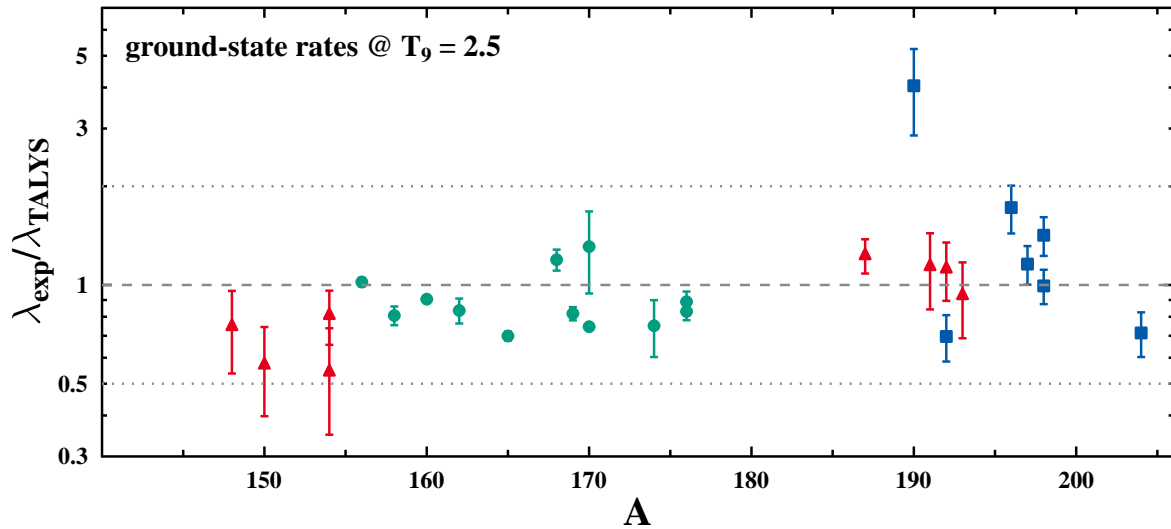


**Figure 6.** Comparison of measured to predicted  $(\gamma, n)$  reaction rates. The ratio of the experimentally determined reaction rate  $\lambda_{\text{exp}}$  to the rate  $\lambda_{\text{TALYS}}$  predicted with the standard settings of the TALYS code [24] is shown. The picture is a compilation of the data described in [25] (blue squares), [26] (red triangles), and [22] (green circles, preliminary). Further details can be found in these references.

#### 4. Conclusions and outlook

Advantages and restrictions of activation experiments were discussed to show their applicability for systematic cross section studies related to  $p$ -process nucleosynthesis. Approaches for the determination of reliable particle-nucleus potentials as well as a systematic study of  $(\gamma, n)$  reaction rates were shown. An interesting approach is also to use neutron-capture reactions for the determination of  $(\gamma, n)$  cross sections as shown in [37, 38].

However, the most interesting reactions concerning the production of the heavy  $p$  nuclei involve unstable nuclei. In most cases, the ratio of the  $(\gamma, n)$  rate to the  $(\gamma, p)$  and  $(\gamma, \alpha)$  rate, respectively, has to be determined. Such a measurement can be carried out at setups like R<sup>3</sup>B at the future FAIR facility if Coulomb dissociation in inverse kinematics is used. First approaches on the determination of  $(\gamma, n)$  rates of different molybdenum isotopes were performed to test the method and yielded promising results [39, 40]. However, to measure  $(\gamma, n)$ ,  $(\gamma, p)$ , and  $(\gamma, \alpha)$  reaction cross sections simultaneously at the future R<sup>3</sup>B setup amendments concerning the detection of the emitted  $\alpha$  particles have to be developed and integrated to the setup.

#### Acknowledgements

The experiments were performed with great support by the accelerator staff at the Nuclear Structure Laboratory of the University of Notre Dame (charged particle induced reactions) and at the S-DALINAC, Darmstadt (photon-induced reactions). We also acknowledge the enormous help during the experiments by the local experimental groups at Notre Dame and Darmstadt. Norbert Pietralla and Achim Richter encouraged the measurements as spokespersons of the SFB 634.

This work is supported by the Deutsche Forschungsgemeinschaft (SFB 634), by the LOEWE program of the State of Hesse (Helmholtz International Center for FAIR), and the German Academic Exchange Service (DAAD). In addition, the National Science Foundation (NSF) and the Joint Institute for Nuclear Astrophysics supported this work.

## References

- [1] Käppeler F 1999 *Prog. Part. Nucl. Phys.* **43** 419
- [2] Käppeler F and Mengoni A 2006 *Nucl. Phys.* **A777** 291
- [3] Dillmann I, Domingo Pardo C, Käppeler F, Mengoni A and Sonnabend K 2008 *Publications of the Astronomical Society of Australia* **25** 18–29
- [4] Wallerstein G, Iben I, Parker P, Boesgaard A M, Hale G M, Champagne A E, Barnes C A, Käppeler F, Smith V V, Hoffman R D, Timmes F X, Sneden C, Boyd R N, Meyer B S and Lambert D L 1997 *Rev. Mod. Phys.* **69** 995
- [5] Lambert D L 1992 *Astron. Astroph. Rev.* **3** 201
- [6] Arnould M and Goriely S 2003 *Phys. Rep.* **384** 1
- [7] Schatz H, Aprahamian A, Görres J, Wiescher M, Rauscher T, Rembges J, Thielemann F K, Pfeiffer B, Möller P, Kratz K L, Herndl H, Brown B and Rebel H 1998 *Phys. Rep.* **294** 167
- [8] Fröhlich C, Martinez-Pinedo G, Liebendörfer M, Thielemann F K, Bravo E, Hix W, Langanke K and Zinner N 2006 *Phys. Rev. Lett.* **96** 142502
- [9] Rapp W, Görres J, Wiescher M, Schatz H and Käppeler F 2006 *Astrophys. J.* **653** 474–489
- [10] Rauscher T 2006 *Phys. Rev. C* **73** 015804
- [11] Farouqi K, Kratz K L, Mashonkina L I, Pfeiffer B, Cowan J J, Thielemann F K and Truran J W 2009 *Astrophys. J.* **694** L49
- [12] Hauser W and Feshbach H 1952 *Phys. Rev.* **87** 366
- [13] Rauscher T and Thielemann F K 2000 *At. Data Nucl. Data Tables* **75** 1
- [14] Rauscher T and Thielemann F K 2004 *At. Data Nucl. Data Tables* **88** 1
- [15] Güray R T, Özkan N, Yalçın C, Palumbo A, deBoer R, Görres J, Leblanc P J, O'Brien S, Strandberg E, Tan W P, Wiescher M, Fülöp Z, Somorjai E, Lee H Y and Greene J P 2009 *Phys. Rev. C* **80** 035804
- [16] Fülöp Z, Gyürky G, Máté Z, Somorjai E, Zolnai L, Galaviz D, Babilon M, Mohr P, Zilges A, Rauscher T, Oberhummer H and Staudt G 2001 *Phys. Rev. C* **64** 065805
- [17] Galaviz D, Fülöp Z, Gyürky G, Máté Z, Mohr P, Rauscher T, Somorjai E and Zilges A 2005 *Phys. Rev. C* **71** 065802
- [18] Kiss G, Fülöp Z, Gyürky G, Máté Z, Somorjai E, Galaviz D, Kretschmer A, Sonnabend K and Zilges A 2006 *Eur. Phys. Journal A* **27** 197–200
- [19] Kiss G G, Mohr P, Fülöp Z, Galaviz D, Gyürky G, Elekes Z, Somorjai E, Kretschmer A, Sonnabend K, Zilges A and Avrigeanu M 2009 *Phys. Rev. C* **80** 045807
- [20] Gyürky G, Kiss G G, Elekes Z, Fülöp Z, Somorjai E, Palumbo A, Görres J, Lee H Y, Rapp W, Wiescher M, Özkan N, Güray R T, Efe G and Rauscher T 2006 *Phys. Rev. C* **74** 025805
- [21] Vogt K, Mohr P, Babilon M, Enders J, Hartmann T, Hutter C, Rauscher T, Volz S and Zilges A 2001 *Phys. Rev. C* **63** 055802
- [22] Müller S 2009 *Bestimmung von Photo-Neutron-Wirkungsquerschnitten in Kernen der Seltenen Erden für den astrophysikalischen p-Prozess mit Bremsstrahlung am S-DALINAC*, doctoral thesis, TU Darmstadt
- [23] Knörzer M 2010 *Untersuchung der Reaktion  $^{166}\text{Er}(\alpha, n)$  mittels Aktivierung*, bachelor thesis, TU Darmstadt, unpublished
- [24] Koning A J, Hilaire S and Duijvestijn M C 2005 vol 769 ed Haight R C, Chadwick M B, Kawano T and Talou P (AIP) pp 1154–1159
- [25] Sonnabend K, Vogt K, Galaviz D, Müller S and Zilges A 2004 *Phys. Rev. C* **70** 035802
- [26] Hasper J, Müller S, Savran D, Schnorrenberger L, Sonnabend K and Zilges A 2008 *Phys. Rev. C* **77** 015803
- [27] Nair C, Erhard M, Junghans A R, Bemmerer D, Beyer R, Grosse E, Klug J, Kosev K, Rusev G, Schilling K D, Schwengner R and Wagner A 2008 *Phys. Rev. C* **78** 055802
- [28] Hasper J, Galaviz D, Müller S, Sauerwein A, Savran D, Schnorrenberger L, Sonnabend K and Zilges A 2009 *Phys. Rev. C* **79** 055807
- [29] Nair C, Junghans A R, Erhard M, Bemmerer D, Beyer R, Grosse E, Kosev K, Marta M, Rusev G, Schilling K D, Schwengner R and Wagner A 2010 *Phys. Rev. C* **81** 055806
- [30] Utsunomiya H, Makinaga A, Goko S, Kaihori T, Akimune H, Ohta M, Yamagata T, Toyokawa H, Lui Y W, Müller S and Goriely S 2006 *Phys. Rev. C* **74** 025806
- [31] Utsunomiya H, Goriely S, Kondo T, Kaihori T, Makinaga A, Goko S, Akimune H, Yamagata T, Toyokawa H, Matsumoto T, Harano H, Hohara S, Lui Y W, Hilaire S, Péru S and Koning A J 2008 *Phys. Rev. Lett.* **100** 162502
- [32] Sonnabend K, Hasper J, Müller S, Pietralla N, Savran D, Schnorrenberger L and Zilges A 2009 vol 1090 ed Jolie J, Zilges A, Warr N and Blazhev A (AIP) pp 481–485
- [33] Utsunomiya H, Mohr P, Zilges A and Rayet M 2006 *Nucl. Phys.* **A777** 459
- [34] Elvers M, Hasper J, Müller S, Savran D, Schnorrenberger L, Sonnabend K and Zilges A 2008 *J. Phys. G* **35** 014027

- [35] Savran D, Lindenberg K, Glorius J, Löher B, Müller S, Pietralla N, Schnorrenberger L, Simon V, Sonnabend K, Wälzlein C, Elvers M, Endres J, Hasper J and Zilges A 2010 *Nucl. Instr. and Meth. A* **613** 232
- [36] Sonnabend K, Savran D, Beller J, Büssing M, Constantinescu A, Elvers M, Endres J, Glorius J, Hasper J, Isaak J, Löher B, Müller S, Pietralla N, Sauerwein A, Schnorrenberger L, Wälzlein C, Zilges A and Zweidinger M 2010 *The Darmstadt High-Intensity Photon Setup (DHIPS)*, *Nucl. Instr. Meth. Phys. Res. A*, submitted
- [37] Dillmann I, Heil M, Käppeler F, Rauscher T and Thielemann F K 2006 *Phys. Rev. C* **73** 015803
- [38] Dillmann I, Domingo-Pardo C, Heil M, Käppeler F, Walter S, Dababneh S, Rauscher T and Thielemann F K 2010 *Phys. Rev. C* **81** 015801
- [39] Sonnabend K, Babilon M, Hasper J, Müller S, Zarza M and Zilges A 2006 *Eur. Phys. Journal A* **27** 149
- [40] Ershova O, Adrich P, Alvarez-Pol H, Aksouh F, Aumann T, Babilon M, Behr K H, Benlliure J, Berg T, Böhmer M, Boretzky K, Brünle A, Beyer R, Casarejos E, Chartier M, Cortina-Gil D, Chatillon A, Pramanik U D, Deveaux L, Elvers M, Elze T W, Emling H, Erhard M, Fernandez-Dominguez B, Geissel H, Gorska M, Heil M, Hellström M, Ickert G, Johansson H, Junghans A R, Käppeler F, Kiselev O, Klimkiewicz A, Kratz J V, Kulesa R, Kurz N, Labiche M, Bleis T L, Lemmon R, Lindenberg K, Litvinov Y, Maierbeck P, Movsesyan A, Müller S, Nilsson T, Nociforo C, Paar N, Palit R, Paschalis S, Prokopowicz W, Reifarth R, Rossi D, Schnorrenberger L, Simon H, Sümmerer K, Surowka G, Vretenar D, Wagner A, Walter S, Walus W, Weick H, Winckler N, Winkler M and Zilges A 2010 vol PoS(NIC-XI) ed Blaum K, Christlieb N and Martínez-Pinedo G (Proceedings of Science) p 232